IOPscience iopscience.iop.org

Home Search Collections Journals About Contact us My IOPscience

The minimum or natural rate of flow and droplet size ejected by Taylor cone–jets: physical symmetries and scaling laws

This content has been downloaded from IOPscience. Please scroll down to see the full text.

2013 New J. Phys. 15 033035

(http://iopscience.iop.org/1367-2630/15/3/033035)

View the table of contents for this issue, or go to the journal homepage for more

Download details:

IP Address: 150.214.182.56
This content was downloaded on 17/12/2014 at 16:21

Please note that terms and conditions apply.

New Journal of Physics
The open access journal for physics

The minimum or natural rate of flow and droplet size ejected by Taylor cone–jets: physical symmetries and scaling laws

A M Gañán-Calvo[1,3], **N Rebollo-Muñoz**[2] **and J M Montanero**[2]

[1] Escuela Superior de Ingenieros, Universidad de Sevilla, Camino de los Descubrimientos s/n, E-41092 Sevilla, Spain
[2] Departamento de Ingeniería Mecánica, Energética y de los Materiales, Universidad de Extremadura, E-06071 Badajoz, Spain
E-mail: amgc@us.es

New Journal of Physics **15** (2013) 033035 (13pp)
Received 20 May 2012
Published 22 March 2013
Online at http://www.njp.org/
doi:10.1088/1367-2630/15/3/033035

Abstract. We aim to establish the scaling laws for both the minimum rate of flow attainable in the steady cone–jet mode of electrospray, and the size of the resulting droplets in that limit. Use is made of a small body of literature on Taylor cone–jets reporting precise measurements of the transported electric current and droplet size as a function of the liquid properties and flow rate. The projection of the data onto an appropriate non-dimensional parameter space maps a region bounded by the minimum rate of flow attainable in the steady state. To explain these experimental results, we propose a theoretical model based on the generalized concept of physical symmetry, stemming from the system time invariance (steadiness). A group of symmetries rising at the cone-to-jet geometrical transition determines the scaling for the minimum flow rate and related variables. If the flow rate is decreased below that minimum value, those symmetries break down, which leads to dripping. We find that the system exhibits two instability mechanisms depending on the nature of the forces arising against the flow: one dominated by viscosity and the other by the liquid polarity. In the former case, full charge relaxation is guaranteed down to the minimum flow rate, while in the latter the instability condition becomes equivalent to

[3] Author to whom any correspondence should be addressed.

Content from this work may be used under the terms of the Creative Commons Attribution-NonCommercial-ShareAlike 3.0 licence. Any further distribution of this work must maintain attribution to the author(s) and the title of the work, journal citation and DOI.

© IOP Publishing Ltd and Deutsche Physikalische Gesellschaft

the symmetry breakdown by charge relaxation or separation. When cone–jets are formed without artificially imposing a flow rate, a microjet is issued quasi-steadily. The flow rate naturally ejected this way coincides with the minimum flow rate studied here. This natural flow rate determines the minimum droplet size that can be steadily produced by any electrohydrodynamic means for a given set of liquid properties.

Contents

1. Introduction **2**
2. Physical symmetries and scaling laws **3**
2.1. Dimensionless groups and characteristic values 3
2.2. System symmetries 5
2.3. Scaling laws for the characteristic quantities 6
2.4. The minimum flow rate 6
2.5. Charge relaxation and separation issues 8
3. Experimental verification **9**
4. Conclusions **11**
Acknowledgments **12**
References **12**

1. Introduction

Taylor cone–jets naturally occur under appropriate circumstances: for example, when a liquid drop is subjected to a strong electric field [3] or a flat liquid interface holds sufficient electric charges [4]. Taylor cones can be sustained for a long time as long as the electric boundary conditions do not change, and the liquid pool where the cone forms is sufficiently large. In this case, a quasi-steady liquid ejection is produced in the form of a *natural* cone–jet, and the issued rate of flow is essentially determined by the liquid properties. This phenomenon exhibits a wealth of physical balances and delicate symmetries, similar to those appearing in other capillary problems such as the pinch-off of an interface [5, 6]. The richness and complexity of electrospray are difficult to find in other fields of meso-scale physics, and long ago attracted the attention of many investigators [7–11]. Among the fields that benefited from an intelligent use of its singular properties, analytical chemistry of biomolecules may be the most salient one [12–15]. Increasingly demanding industry standards of sensitivity, discrimination, etc have motivated researchers to deepen the physical mechanisms involved in this phenomenon [16–18], fruitfully merging varied research fields.

The range of applied voltages (electric fields) necessary to produce Taylor cone–jets is very narrow. It depends on the boundary conditions and geometry of the domain where the liquid drop sits, and is determined by the existence of an underlying static solution with a conical peak for the tapering meniscus [19–23]. Before emission takes place, there is a critical value of the applied electric field above which the drop develops an instability [20, 21] leading to a conical shape. Similarly, in the case of an isolated or suspended liquid drop in a gas or vacuum, two opposite Taylor cones pointing in the electric field direction are formed at a critical applied electric field [24–26]. For drops attached to a given boundary, there is a univocal

relationship between the applied voltage and the volume of the resulting static liquid meniscus with a Taylor peak, as shown in [22]. This peak constitutes a singularity smoothed out by a small liquid ejection. The liquid ejection entails the spread of electric charge in front of the cone tip. The presence of this charge reduces the electric field intensity at the conical tip, and thus the meniscus elongates and relaxes. To produce a Taylor cone–jet, one can fix the applied voltage first, and then add or extract liquid to accommodate the meniscus volume/shape to the prescribed voltage.

In the phenomenon described above, the ejected flow rate is a function of the boundary conditions, the applied voltage and, more importantly, the liquid properties. This *natural* flow rate is that satisfying a set of physical symmetries taking place at the meniscus tip. However, one can 'stretch' those symmetries by imposing a certain flow rate above the natural one. Larger imposed flow rates lead to larger issued jets, and thus larger resulting droplets. The surface charge is essentially determined by the liquid properties [27], and thus both the electric current transported by the Taylor cone–jet [28, 29] and the space charge due to the issued spray [30] also increase with the flow rate. This explains why the conical meniscus elongates under the same applied electric field when the prescribed flow rate is increased.

It must be noted that the steady cone–jet mode cannot be reached by imposing a flow rate smaller than the natural one. In that case, the liquid ejected by the Taylor cone would not be replaced, the meniscus volume would decrease progressively, moving away from that of the underlying static solution, and the jet emission would be eventually interrupted. One concludes that the liquid flow rate naturally issued by a Taylor cone–jet is also the minimum flow rate that can be steadily ejected for the same liquid. Therefore, the natural flow rate determines the minimum size of the droplets steadily produced by electrospraying.

In this work, we will ascertain the value of the minimum flow rate that can be steadily issued by a Taylor cone–jet as a function of the liquid properties. Our analysis will be based only on rather general assumptions (such as the locality of the cone–jet transition region). In particular, we will not resort to hypotheses on charge relaxation, although recent numerical simulations [31] have pointed to a nearly complete charge relaxation in all the cases considered.

2. Physical symmetries and scaling laws

2.1. Dimensionless groups and characteristic values

The parameters that essentially characterize the steady cone–jet mode are: (i) the issued rate of flow Q, (ii) the liquid properties (density ρ, surface tension σ, viscosity μ, electrical conductivity K and electrical permittivity ε_i) and (iii) the outer environment properties. We shall assume that the outer environment is either vacuum or a low-viscosity dielectric fluid [32], and thus its dynamical effect on the system can be neglected. In this case, the only parameter characterizing its influence is its electrical permittivity ε_o. The applied voltage V is left out of the analysis because, as discussed in the introduction, it must be that necessary for achieving the underlying static solution which supports the steadily ejecting tip. Furthermore, the jet emission in the steady cone–jet mode relies on the singular fluidic structure arising in the cone–jet transition region. The characteristic length of this region is much smaller than those characterizing the electrospray device. Because of the locality of the cone–jet transition, the steady cone–jet mode losses its dependence on the device geometrical features and associated lengths [23, 33].

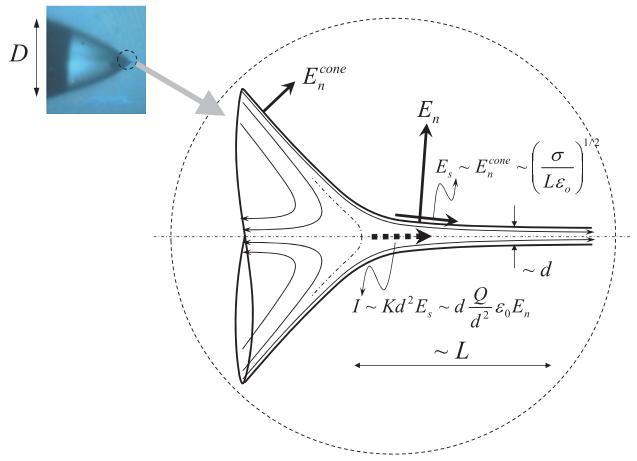

Figure 1. Schematics of the Taylor cone–jet situation at the minimum rate of issued flow.

The physical variables defining univocally the state of the system are the interface position $r = \hat{f}(z)$ (r and z are the radial and axial cylindrical coordinates, respectively), as well as the velocity $\hat{\mathbf{v}}_{\mathrm{i,o}}$ and electric fields $\hat{\mathbf{E}}_{\mathrm{i,o}}$ inside and outside the liquid (the subindexes i and o stand for the inner and outer domains, respectively). Observe that we do not take note of the issued electric current $\hat{I}$ since this is a secondary quantity determined by the primary variables mentioned above. The general equations governing the relationship among these variables are well known (see e.g. [23, 33]) and will not be repeated here.

The minimum flow rate Q^* ejected in the steady cone–jet mode is a function of the governing parameters mentioned above, i.e. $Q^* = Q^*(\rho, \mu, \sigma, K, \varepsilon_{\mathrm{i}}, \varepsilon_{\mathrm{o}})$. This relationship can be expressed in terms of three dimensionless groups [34]:

$$\frac{Q^*}{Q_{\mathrm{o}}} = G(\delta_\mu, \beta)\,, \tag{1}$$

where $Q_{\mathrm{o}} = \sigma\varepsilon_{\mathrm{o}}/(\rho K)$ [23, 27, 29, 30, 33, 35], $\delta_\mu = [\sigma^2\rho\varepsilon_{\mathrm{o}}/(\mu^3 K)]^{1/3}$ (also definable as the electrohydrodynamic Reynolds number) and $\beta = \varepsilon_{\mathrm{i}}/\varepsilon_{\mathrm{o}}$. One searches for a similarity or scaling law for equation (1), $G = \delta_\mu^{\alpha_1}\beta^{\alpha_2}$, where $\alpha_{1,2}$ can take any rational values[4].

Let us define d, U, E_{s}, E_{n} and I as the characteristic values of the interface position (jet radius), the liquid axial velocity, the tangential and normal electric fields on the liquid surface and the issued electric current, respectively. One assumes that there is a region of the liquid domain where all those quantities are of the order of their corresponding characteristic values. That electrohydrodynamic region is delimited by the axial characteristic length L (see figure 1). The electrohydrodynamic region typically, but not necessarily, corresponds to the cone–jet region.

The equilibrium of electric forces in the cone yields the Taylor's solution [19, 22, 23], which allows one to calculate the characteristic value of the tangential electric field

$$E_{\mathrm{s}} = \left(\frac{\sigma}{\varepsilon_{\mathrm{o}}L}\right)^{1/2}. \tag{2}$$

This value also characterizes the normal electric field on the surface of the conical region.

[4] Possible values of $\alpha_{1,2}$ are restricted to rational numbers on the basis of dimensional analysis (Vaschi–Buckingham Π-theorem) for a finite number of fundamental parameters, variables and governing equations.

The relationships between the above characteristic quantities can be ascertained through an analysis of the balance of mass, momentum, energy and electric charge occurring in the local cone–jet region [34]. Interestingly, the concept of 'symmetry' can be applied to these balances independent of time, and thus any particular balance can be regarded as a 'symmetry' of the system stemming from time invariance.

2.2. System symmetries

Consider an electrospray realization in which the flow rate Q is a prescribed parameter (a common practice in electrospraying). Here, we seek the relationships between the characteristic quantities $\{d, E_s, E_n, U, I, L\}$ involving the governing parameters $\{\rho, \mu, \sigma, K, \varepsilon_i, \varepsilon_o\}$ and the imposed flow rate Q.

The smallness of the jet's diameter forces a rapid radial diffusion of momentum from the surface, even for the lowest viscosities tested in practice (e.g. light alkanes such as hexane or heptane). This occurs in spite of the fact that the axial velocity can be significantly distorted in the radial direction at the cone–jet neck [36]. Therefore, mass conservation allows one to establish the first symmetry for the characteristic liquid velocity

$$U = Q\, d^{-2}. \tag{3}$$

The second symmetry can be found from the axial momentum equation as applied to the electrohydrodynamic region [27]. The terms of that equation can be grouped into *driving* and *resistant* forces per unit volume. The first group is

$$\{\varepsilon_o E_n^2 L^{-1},\ \varepsilon_o \beta E_s^2 L^{-1},\ \varepsilon_o E_n E_s d^{-1}\}\,. \tag{4}$$

Here, these terms are generally referred to as the electrostatic, polar and electric tangential forces, respectively [27]. To calculate these terms, we have considered that $\beta - 1 \simeq \beta$, and the normal component of the electric field on the outer side of the interface is much larger than that on the inner side [27]. The second group comprises the terms

$$\{\sigma d^{-1} L^{-1},\ \rho Q^2 d^{-4} L^{-1},\ \mu Q\, d^{-2} L^{-2}\} \tag{5}$$

which correspond to surface tension, inertia and viscosity, respectively. Both numerical and experimental studies have shown that the polarization force $\varepsilon_o \beta E_s^2 L^{-1}$ is at most comparable to the electrostatic force $\varepsilon_o E_n^2 L^{-1}$ [27]. The electric tangential force $\varepsilon_o E_n E_s d^{-1}$ is much smaller than the electrostatic one throughout the cone–jet region, although it is the only force which remains positive when the jet is fully developed [27, 33, 34]. On the other hand, the viscosity force is at most comparable with inertia, while the role played by surface tension is negligible in most cases. The equilibrium between the dominant driving and resistant forces leads to the second symmetry

$$\rho Q^2 d^{-4} = \varepsilon_o E_n^2. \tag{6}$$

The electric power consumed by the system is mostly invested in the kinetic energy of the ejected liquid [34]. In fact, the heat generated by the Joule effect is at most comparable with that kinetic energy. If the liquid were static, then it would heat up as a result of the charge motion through the bulk. However, the 'wire' in electrospray (the jet's bulk) is continuously withdrawn at a high speed by the voltage decay, and thus the basic output of that voltage decay is kinetic

energy, and not heat. The electric power consumed by the system is $IV = K\,d^2 E_s (L\,E_s)$. Taking into account the value of E_s given by (2), one obtains the third symmetry

$$\frac{\sigma}{\varepsilon_o} K\,d^2 = \rho Q^3 d^{-4}. \tag{7}$$

One can assume that conduction gives way to a dominant charge convection over the liquid surface within the electrohydrodynamic region [23, 27, 37]. This assumption allows one to establish the last symmetry:

$$K\,d^2 E_s = \varepsilon_o E_n Q\,d^{-1}. \tag{8}$$

Equations (3) and (6)–(8) constitute the system symmetries characterizing the steady cone–jet regime in electrospray. An interesting feature of this set of symmetries is its independence with respect to the characteristic electrohydrodynamic length L.

2.3. Scaling laws for the characteristic quantities

Some useful scaling laws can be straightforwardly obtained from the system symmetries derived in the previous section. Symmetries (3) and (7) provide the scaling laws for the jet's diameter and velocity:

$$d = d_o (Q/Q_o)^{1/2} \quad \text{and} \quad U = \left(\frac{\sigma K}{\rho \varepsilon_o}\right)^{1/3}, \tag{9}$$

where $d_o = [\sigma \varepsilon_o^2/(\rho K^2)]^{1/3}$ [23, 27, 34]. Equations (6) and (9) lead to the scaling for E_n:

$$E_n = \left(\frac{\sigma^2 \rho K^2}{\varepsilon_o^5}\right)^{1/6}. \tag{10}$$

From this result and equation (8), one obtains

$$E_s = E_n (Q/Q_o)^{-1/2}. \tag{11}$$

Equations (7), (9) and (10) yield the scaling law for the current intensity

$$I = (\sigma K Q)^{1/2} = I_o (Q/Q_o)^{1/2}, \tag{12}$$

where $I_o = \sigma \rho^{-1/2} \varepsilon_o^{1/2}$ [23, 27, 33, 34, 37]. Finally, equations (2) and (11) allow one to obtain a scaling law for the axial characteristic length L:

$$L = d_o (Q/Q_o). \tag{13}$$

From these findings note that the main driver is not only the electrostatic force $\varepsilon_o E_n^2 L^{-1}$ arising from the cone–jet transition region, but also the electric tangential force $\varepsilon_o E_n E_s d^{-1}$ acting along the whole jet.

It is worth noting that the above scaling laws cannot be applied to electrospinning, where viscous forces cannot be neglected even for large flow rates [29]. Besides, the locality of the phenomenon analyzed here demands the characteristic electrohydrodynamic length L to be at most comparable with the characteristic size D of the feeding capillary. Thus, the cases where $D < L$ (e.g. 'nano-electrospray' [38, 39]) are excluded from this analysis.

2.4. The minimum flow rate

Now, a question arises as to what different scenarios would be found if Q were quasi-steadily decreased from the basic asymptotic regime described above. Experience shows that one reaches

a point where the system becomes unstable and drips. The instability can be localized either in the conical meniscus (global instability) or in the jet close to the cone–jet transition region (local instability). We are interested in the absolute minimum value of the flow rate that can be ejected in the steady regime, independently of the instability localization. As explained in the introduction, this value is also the flow rate naturally and steadily extracted when an electric voltage is applied on a liquid interface to form a Taylor cone [25].

Close to the minimum flow rate stability limit, the system symmetries derived in section 2.2 fail to describe the jet emission. Two forces are expected to rise against the electric tangential force as the system approaches its stability limit. The first one is the viscous force appearing at the jet inception. This force may become comparable with inertia as the flow rate decreases. In this case, viscous dissipation prevents the jet from being formed for small enough values of the flow rate, even before the surface tension stalls the jet production [34].

The second instability mechanism is associated with the polarization force appearing beyond the cone–jet transition. This force may become negative in that region for sufficiently small values of the flow rate [27]. Under certain conditions, the driver is unable to overcome the reactive polarization force, and the jet emission is no longer stable. It must be noted that the electrostatic force may also constitute a resistant force beyond the cone–jet transition when the flow rate is very close to its minimum value [27]. However, its magnitude scales as Q (as occurs with the main driver $\varepsilon_o E_n E_s d^{-1}$), while the polarization force scales as $Q^{-1/2}$, and thus the latter becomes the major obstacle in this stability limit.

One finds, therefore, two scenarios when the flow rate approaches its minimum value:

1. *Viscous forces stall the jet emission before polarization forces*. In this case,

$$\mu Q^* d^{-2} L^{-2} = \varepsilon_o E_n^2 L^{-1}. \tag{14}$$

   From this equation and (13), one concludes that the minimum flow rate Q^* and jet diameter d^* scale as

$$Q^* = Q_o \delta_\mu^{-1} \quad \text{and} \quad d^* = d_o \delta_\mu^{-1/2}. \tag{15}$$

2. *Polarization forces rise against the main driver first*. In this case,

$$\varepsilon_o \beta E_s^2 L^{-1} = \varepsilon_o E_n^2 L^{-1}. \tag{16}$$

   Taking into account the scaling laws (10) and (11) for E_n and E_s, respectively, one has that the minimum flow rate and jet diameter should scale as

$$Q^* = Q_o \beta \quad \text{and} \quad d^* = d_o \beta^{1/2}. \tag{17}$$

Equations (15) and (17) allow one to conclude that the parameter $\beta\delta_\mu$ determines which mechanism dominates the minimum flow rate instability: for $\beta\delta_\mu < 1$ the loss of stability is caused by the viscous forces, while polarization forces are responsible for instability for $\beta\delta_\mu > 1$. It must be noted that the conditions $Q > Q_o \delta_\mu^{-1}$ and $\beta\delta_\mu < 1$ are equivalent to those defining the 'IE' (inertia + electrostatic force) regime defined in [35].

As explained in the introduction, the minimum flow rate that can be steadily ejected in electrospraying is also the flow rate naturally and steadily issued by a Taylor cone–jet formed by the same liquid. Therefore, expressions (15) and (17) provide the scales of the flow rate and (diameter of) the jet quasi-steadily ejected by a Taylor cone–jet in the absence of an imposed rate of flow. Both the scaling laws and the dimensionless number $\beta\delta_\mu$ are functions of the liquid properties only.

The literature on the breakup of electrified capillary jets, in conditions comparable with those issued from steady cone–jets (see e.g. [1], section 5 and figure 14 of that classic work, and more recently [2]), supports that the emitted drop is commensurate with the jet, and thus the drop scales as d^* as well. This is particularly true close to the minimum flow rate, for which the electrical Weber numbers of the jet are smaller (see [34, 37]). Thus, in the following, d^* will refer to the scale of both the jet and the droplet diameters indistinguishably.

Basaran and co-workers described in [4] an essentially *unsteady* phenomenon. They derived the scaling laws governing the size of the *first* ejected droplet when a liquid interface is suddenly electrified and tapers a microjet. In contrast, the symmetries invoked in the present work are based on time invariance, and thus the scaling laws (9)–(13) cannot be applied to that problem. The analyses presented in [4] and here can be regarded as complementary studies to describe electrospray tip streaming, but they are separated by a fundamental barrier: system steadiness.

To clarify the above statement, the scaling for the drop size here obtained is compared with that reported in [4] for the *first* issued drop: $d_B \sim d_o \beta^{1/3} \delta_\mu^{-1}$. When viscous forces arise first, $d^*/d_B = \beta^{-1/3}\delta_\mu^{1/2} = \beta^{-5/6}\left(\beta\delta_\mu\right)^{1/2}$, while in the polarization case $d^*/d_B = \beta^{1/6}\delta_\mu = \beta^{-5/6}\left(\beta\delta_\mu\right)$. In both cases, the factor $\beta^{-5/6}$ appears in combination with the critical parameter $\beta\delta_\mu$. The discrepancy between d^* and d_B reflects the influence of charge relaxation/separation on the initial stage of liquid ejection. A detailed analysis of the charge relaxation/separation processes is beyond the scope of this work. In section 2.5, the characteristic time $t_e \sim \beta\varepsilon_o/K$ associated with charge relaxation is compared with the hydrodynamic time characterizing our steady process to assess the consistency of our scaling laws.

2.5. *Charge relaxation and separation issues*

Charge relaxation phenomena take place when the characteristic time t_e of charge diffusion under an applied electric field becomes comparable with the smallest characteristic hydrodynamic time of the system. In steady cone–jet electrospraying, the smallest hydrodynamic time is given by the characteristic residence time in the electrohydrodynamic region, $t_h \sim L/U = d^2 L/Q$. Two possibilities can be contemplated:

1. The case $\beta\delta_\mu < 1$ (viscous force arises first when the system operates near the minimum flow rate stability limit). Equations (14) and (15) allow one to calculate the ratio of the electrical relaxation time to the hydrodynamic time

$$t_e/t_h \sim \beta \frac{\varepsilon_o Q^*}{K d^{*2} L} = \beta \frac{\delta_\mu^{-1}}{\delta_\mu^{-1-1}} = \beta\delta_\mu. \tag{18}$$

   Therefore, the minimum flow rate Q^* is reached *before* any 'choking' charge relaxation phenomena arise.

2. The case $\beta\delta_\mu > 1$ (polarization force arises first when the system operates near the minimum flow rate stability limit). From equations (17), one concludes that

$$t_e/t_h \sim \beta \frac{\beta^1}{\beta^{1+1}} = 1. \tag{19}$$

   In this case, polarization forces oppose the flow concomitantly when charge relaxation and separation phenomena take place. Observe that this limit implies the same assumptions as

those made in [29] for the entire flow rate range. However, we show that these assumptions can only be made in the limit of minimum flow rate for $\beta\delta_\mu > 1$.

The above results show that charge relaxation in steady cone–jet electrospraying is at least as fast as any hydrodynamic processes taking place in the system. In fact, if the charge supply to the jet interrupts at any point of the cone–jet transition, then time-invariance would break down, the system would reach an unsustainable state, and steady jetting would no longer be possible. Thus, models that explain the physics of steady Taylor cones involving phenomena such as complete charge separation or surface charge freezing at the cone–jet transition [29, 40] need revision.

A precise description of the limiting situations considered in this work requires either a numerical resolution of all the equations [41] or the use of appropriate prefactors in the scaling laws. The experimental analysis accomplished in section 3 will enable us to confirm the validity of our predictions and provide information about those prefactors.

3. Experimental verification

We make use of experimental results gathered from a small body of literature on the subject [29, 42–45],[5] consisting of 15 series of experiments (see table 1) where the authors, as far as we know, drove their setups down to the minimum flow rates that their equipment allowed. Details and discussions of the experiments can be seen in the respective references. Also, we conducted experiments to cover intermediate values of the parameter $(\beta\delta_\mu)^{-1}$. In our experiments, the liquid was injected at a constant flow rate through a capillary of inner (outer) radius 100 (110) μm located in front of a metallic plate at a distance of 1 mm. An electric potential was applied to the end of the feeding capillary through a dc high-voltage power supply, while the plate was used as the ground electrode. A liquid meniscus was formed in the open air and stretched by the action of the electric field. A microjet tapered from the meniscus tip and moved vertically toward the plate. Digital images were acquired to check that the fluid configuration was steady. The liquid flow rate Q was reduced in steps of 0.1 ml h^{-1} until the dripping regime was reached.

Figure 2 shows the ratio $Q/(Q_\mathrm{o}\beta)$ as a function of $(\beta\delta_\mu)^{-1}$. For $(\beta\delta_\mu)^{-1} > 1$, the minimum flow rate is essentially independent of β over two orders of magnitude of the parameter $(\beta\delta_\mu)^{-1}$. This interval is bounded by the data obtained by Gamero-Castaño [44],[6] which correspond to the smallest value of δ_μ found in the literature. The minimum value of $Q/(Q_\mathrm{o}\delta_\mu^{-1})$ is approximately unity for all the liquids of this interval, and thus the validity of the scaling law (15) is shown even for large values of δ_μ.

For $(\beta\delta_\mu)^{-1} < 1$, Q^* is proportional to both Q_0 and β, as predicted by (17). The data obtained by Hayati *et al* [43] provide a solid support for our theoretical predictions. That series follows the same trend as the others, even though the liquid electrical permittivity in that case is much smaller than in the others. A paradigmatic case is that of Guerrero *et al* [45], which exhibits the largest electrical permittivity of all the series. Their work presents with caution experiments with extremely small flow rates. They suspect both changes in the liquid properties due to differential evaporation of the solvent in their mixtures, and almost complete suppression of liquid ejection owing to ion emission (these conditions correspond to the outlier point in

[5] Experiments conducted in the present work.

[6] Professor Gamero-Castaño kindly provided the author with two extra values of extreme low flow rates not reported in his paper.

Table 1. Properties of the liquids used in the experimental series.

Liquid	Reference	ρ (kg m^{-3})	σ (N m^{-1})	β	K (S m^{-1})	μ (Pa s)
Ethyl. glyc. 2	[29]	1110	0.0484	38.66	6.26×10^{-2}	0.021
Ethyl. glyc. 3	[29]	1110	0.0484	38.66	1.69×10^{-2}	0.021
3-Ethyl. glyc. (b)	[42]	1134	0.0454	23.7	1.27×10^{-3}	0.0366
3-Ethyl. glyc. (c)	[42]	1134	0.0454	23.7	2.73×10^{-3}	0.0366
3-Ethyl. glyc. (d)	[42]	1134	0.0454	23.7	5.04×10^{-3}	0.0366
3-Ethyl. glyc. (e)	[42]	1134	0.0454	23.7	1.58×10^{-2}	0.0366
4-Ethyl. glyc. (a)	[42]	1137	0.0448	20.5	7.38×10^{-3}	0.0456
4-Ethyl. glyc. (b)	[42]	1137	0.0448	20.5	3.70×10^{-2}	0.0456
Isopar + 15% n-butOH	[43]	754.75	0.024	2.64	7.14×10^{-9}	0.00173
EMI-Im	[44]	1520	0.0349	3	8.80×10^{-1}	0.034
PC-EMI-BF4	[45]	1200	0.042	65	1.04	0.00276
1-Octanol	See footnote 4	827	0.027	10	9.0×10^{-7}	0.0081
1-Decanol	See footnote 4	828	0.028	7.6	3.0×10^{-7}	0.01179
1-Dodecanol	See footnote 4	830	0.0275	6.5	1.0×10^{-7}	0.0125
3-Ethyl glyc.	See footnote 4	1120	0.0454	23.7	0.0011	0.0401

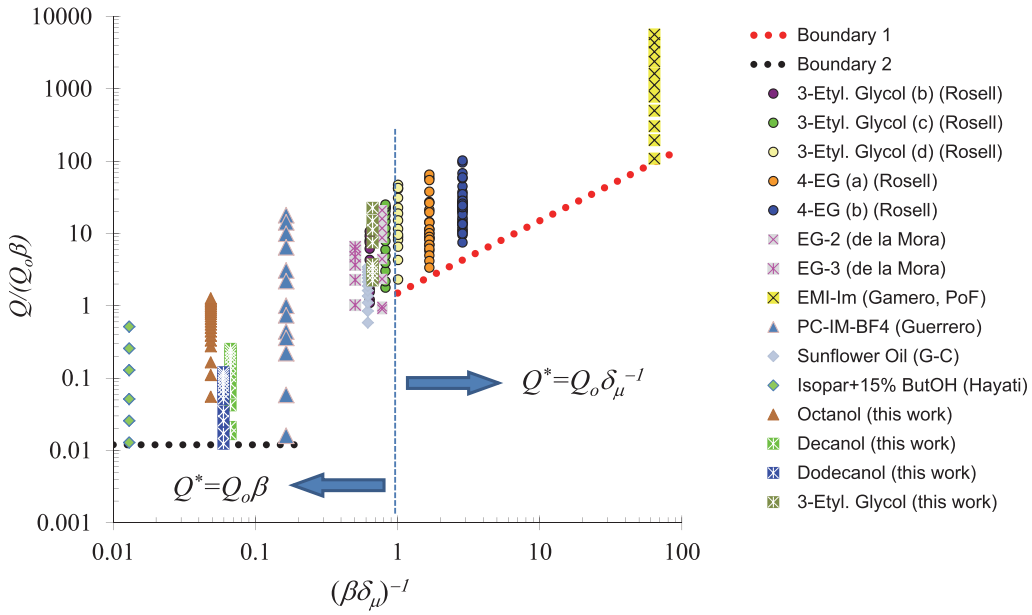

Figure 2. $Q/(Q_o\beta)$ as a function of $(\beta\delta_\mu)^{-1}$. Details of the experimental series are given in their corresponding references (see table 1).

this series). In spite of this, their results agree remarkably well with the general trend for the $(\beta\delta_\mu)^{-1} < 1$ range.

It must be noted that the minimum values of $Q/(Q_o\beta)$ for $(\beta\delta_\mu)^{-1} < 1$ are hardly above 0.01. This effect can be explained as follows. Our scaling analysis indicates that $\beta E_s^2/E_n^2 = \beta Q_o/Q$ in this regime. However, the experiments show that the maximum values of the polarization and electrostatic forces are about $0.09^2 \times \beta\varepsilon_o E_s^2$ and $0.5^2 \times \varepsilon_o E_n^2$, respectively (see [27], p 868, figure 2). This yields a maximum value for the ratio $\beta E_s^2/E_n^2$ of about

$(0.09/0.5)^2 = 0.032$. Thus, one may expect the system reaching flow rates significantly below βQ_o to have a noticeable rise of the polarization forces.

It must also be noted that the minimum flow rate plunges below $Q_o\delta_\mu^{-1}$ for $(\beta\delta_\mu)^{-1} \lesssim 1$. A plausible explanation of this effect may be the following. Charge continuity in the cone–jet transition region demands that the axial electric field increases as the cone–jet cross section decreases. Thus, the polarization force in this region points in the downstream direction. However, the axial electric field given by the Taylor solution decreases downstream from a certain location where it reaches a maximum [33, 46]. When $(\beta\delta_\mu)^{-1}$ becomes small, the polarization forces in the cone–jet transition region become comparable with the driving force, providing the liquid with an *additional* push in that critical region. This occurs even though polarization forces act against the flow when the jet is developed. This initial push may result in an extra stabilization of the system for $(\delta_\mu\beta)^{-1} \lesssim 1$, which allows one to reach flow rates as small as $0.01 \times Q_o\beta$, well below $Q_o\delta_\mu^{-1}$. For flow rates below $0.01 \times Q_o\beta$, the negative action of the polarization forces and, possibly more importantly, charge separation [41] preclude the existence of steady jetting.

4. Conclusions

In this work, we obtained the scaling laws for the minimum flow rate attainable by the steady cone–jet configuration. This quantity coincides with the flow rate naturally ejected by quasi-steady Taylor cone–jets, and determines the minimum size of the droplets steadily produced by electrospraying. The scaling laws for the minimum flow rate were obtained by considering a system of symmetries stemming from time invariance, and valid for the cone–jet transition of the steady mode. If the flow rate is decreased below its threshold value, those symmetries break down, and the cone–jet regime becomes globally unstable. Our analysis relies on general assumptions, and does not assume any hypotheses on the charge relaxation process occurring in the electrified liquid.

The minimum flow rate obeys two different scaling laws depending on the nature of the force opposing the liquid motion. If the viscosity force is responsible for instability, the minimum flow rate is given by equation (15), while equation (17) applies when the polarization force destabilizes the cone–jet mode. Interestingly, in the first case full charge relaxation is guaranteed down to the minimum flow rate, while in the second limit the charge relaxation/separation condition also breaks down. Both the experimental results gathered from the literature and those conducted in this work show the validity of our predictions. The results presented in this paper have obvious technological applications, because they allow one to determine the minimum droplet size that can be reached by electrohydrodynamic means for a given set of liquid properties.

One of the aspects of electrospraying which deserves attention is the transition taking place from the very first stage of the liquid ejection to the subsequent quasi-steady flow occurring once that ejection is established. The differences between the flow rates and jet diameters characterizing those two processes must reveal the role played by charge relaxation/separation in electrospraying. To visualize what happens just after the liquid ejection, it would be very beneficial to combine full numerical simulations (including a detailed electro-kinetic model) with experiments conducted with a sufficiently high spatio-temporal resolution.

Acknowledgments

Partial support from the Ministry of Science and Education (Spain) through grant no. DPI2010-21103-C04 for this work is acknowledged. The valuable feedback from an anonymous referee is also acknowledged. AMGC conducted the study, wrote the paper and compiled the results from the literature. JMM and NRM performed the experiments.

References

[1] Cloupeau M and Prunet-Foch B 1989 Electrostatic spraying of liquids in cone–jet mode *J. Electrostat.* **22** 135–59
[2] López-Herrera J M and Gañán-Calvo A M 2004 A note on charged capillary jet breakup of conducting liquids: experimental validation of a viscous one-dimensional model *J. Fluid Mech.* **501** 303–26
[3] Gomez A and Tang K 1994 Charge and fission of droplets in electrostatic sprays *Phys. Fluids* **6** 404–14
[4] Collins R T, Jones J J, Harris M T and Basaran O A 2008 Electrohydrodynamic tip streaming and emission of charged drops from liquid cones *Nature Phys.* **4** 149–54
[5] Eggers J 1997 Nonlinear dynamics and breakup of free-surface flows *Rev. Mod. Phys.* **69** 865–929
[6] Eggers J and Villermaux E 2008 Physics of liquid jets *Rep. Prog. Phys.* **71** 036601
[7] Zeleny J 1914 The electrical discharge from liquid points and a hydrostatic method of measuring the electric intensity at their surfaces *Phys. Rev.* **3** 69–91
[8] Zeleny J 1917 Instability of electrified liquid surfaces *Phys. Rev.* **10** 1–6
[9] Carswell D J and Milsted J 1957 A new method for the preparation of thin films of radioactive material *J. Nucl. Energy* **4** 51–4
[10] Michelson D and Richardson H O W 1963 A note on making thin β-ray sources by electrostatic spraying *Nucl. Instrum. Methods* **21** 355
[11] Shorey J D and Michelson D 1969 On the mechanism of electrospraying *Nucl. Instrum. Methods* **82** 295–6
[12] Fenn J B, Mann M, Meng C K, Wong S F and Whitehouse C M 1989 Electrospray ionization for mass spectrometry of large biomolecules *Science* **246** 64–71
[13] Marginean I, Nemes P and Vertes A 2007 Laser ablation electrospray ionization for atmospheric pressure, in vivo and imaging mass spectrometry *Anal. Chem.* **79** 8098–106
[14] Ifa D R, Wu C P, Ouyang Z and Cooks R G 2010 Desorption electrospray ionization and other ambient ionization methods: current progress and preview *Analyst* **135** 669–81
[15] Harris G A, Galhena A S and Fernandez F M 2011 Ambient sampling/ionization mass spectrometry: applications and current trends *Anal. Chem.* **83** 4508–38
[16] Marginean I, Nemes P and Vertes A 2006 Order–chaos–order transitions in electrosprays: the electrified dripping faucet *Phys. Rev. Lett.* **97** 064502
[17] Marginean I, Nemes P and Vertes A 2006 How much charge is there on a pulsating Taylor cone? *Appl. Phys. Lett.* **89** 064104
[18] Nemes P, Marginean I and Vertes A 2007 Spraying mode effect on droplet formation and ion chemistry in electrosprays *Anal. Chem.* **79** 3105–16
[19] Taylor G I 1964 Disintegration of water drops in a electric field *Proc. R. Soc. Lond.* A **280** 383–97
[20] Basaran O A and Scriven L E 1990 Axisymmetric shapes and stability of pendant and sessile drops in an electric field *J. Colloid Interface Sci.* **140** 10–30
[21] Harris M T and Basaran O A 1993 Capillary electrohydrostatics of conducting drops hanging from a nozzle in an electric field *J. Colloid Interface Sci.* **161** 389–413
[22] Pantano C, Gañán-Calvo A M and Barrero A 1994 Zeroth order, electrohydrostatic solution for electrospraying in cone–jet mode *J. Aerosol Sci.* **25** 1065–77
[23] Gañán-Calvo A M 1997 Cone–jet analytical extension of Taylor's electrostatic solution and the asymptotic universal scaling laws in electrospraying *Phys. Rev. Lett.* **79** 217–20

[24] Tsampoulos J A, Akylas T R and Brown R A 1985 Dynamics of charged drop break-up *Proc. R. Soc. Lond.* A **401** 67–88
[25] Stone H A, Lister J R and Brenner M P 1999 Drops with conical ends in electric and magnetic fields *Proc. R. Soc. Lond.* A **455** 329–47
[26] Duft D, Achtzehn T, Müller R, Huber B A and Leisner T 2003 Rayleigh jets from levitated microdroplets *Nature* **421** 128
[27] Gañán-Calvo A M 1999 The surface charge in electrospraying: its nature and its universal scaling laws *J. Aerosol Sci.* **30** 863–72
[28] Gañán-Calvo A M, Barrero A and Pantano C 1993 The electrohydrodynamics of electrified conical menisci *J. Aerosol Sci.* **24** (S1) S19–20
[29] de la Mora J F and Loscertales I G 1994 The current emitted by highly conducting Taylor cones *J. Fluid Mech.* **260** 155–84
[30] Gañán-Calvo A M, Lasheras J C, Dávila J and Barrero A 1994 The electrostatic spray emitted from an electrified conical meniscus *J. Aerosol Sci.* **24** 1121–42
[31] Herrada M A, López-Herrera J M, Gañán-Calvo A M, Vega E J, Montanero J M and Popinet S 2012 Numerical simulation of electrospray in the cone–jet mode *Phys. Rev.* E **86** 026305
[32] Barrero A, Lopez-Herrera J M, Boucard A, Loscertales I G and Marquez M 2004 Steady cone–jet electrosprays in liquid insulator baths *J. Colloid Interface Sci.* **272** 104–8
[33] Higuera F 2003 Flow rate and electric current emitted by a Taylor cone *J. Fluid Mech.* **484** 303–27
[34] Gañán-Calvo A M and Montanero J M 2009 Revision of capillary cone–jet physics: electrospray and flow focusing *Phys. Rev.* E **79** 066305
[35] Gañán-Calvo A M 2004 On the general scaling theory for electrospraying *J. Fluid Mech.* **507** 203–12
[36] Gordillo J M, Pérez-Saborid M and Gañán-Calvo A M 2001 Linear stability of co-flowing liquid–gas jets *J. Fluid Mech.* **448** 23–51
[37] Gañán-Calvo A M, Dávila J and Barrero A 1997 Current and droplets size in the electrospraying of liquid. Scaling laws *J. Aerosol Sci.* **28** 249–75
[38] Carlier J, Arscott S, Thomy V, Camart J-C, Cren-Olivé C and Le Gac S 2005 Integrated microfabricated systems including a purification module and an on-chip nano electrospray ionization interface for biological analysis *J. Chromatogr.* A **1071** 213–22
[39] Arscott S, Le Gac S and Rolando C 2005 A polysilicon nanoelectrospray-mass spectrometry source based on a microfluidic capillary slot *Sensors Actuators* B **106** 741–9
[40] de la Mora J F 2007 The fluid dynamics of Taylor cones *Annu. Rev. Fluid. Mech.* **39** 217–43
[41] Higuera F 2009 Charge separation in the conical meniscus of an electrospray of a very polar liquid: its effect on the minimum flow rate *Phys. Fluids* **21** 032104
[42] Rosell-Llompart J and Fernandez de la Mora J 1994 Generation of monodisperse droplets 0.3 to 4 μm in diameter from electrified cone–jets of highly conducting and viscous liquids *J. Aerosol Sci.* **25** 1093–119
[43] Hayati I, Bailey A I and Tadros Th F 1987 Investigations into the mechanisms of electrohydrodynamic spraying of liquids: I. Effect of electric field and the environment on pendant drops and factors affecting the formation of stable jets and atomization *J. Colloid Interface Sci.* **117** 205–21
[44] Gamero-Castaño M 2008 Characterization of the electrosprays of 1-ethyl-3-methylimidazolium bi(trifluoromethylsulfonyl)imide in vacuum *Phys. Fluids* **20** 032103 1–11
[45] Guerrero I, Bocanegra R, Higuera F J and de la Mora J F 2007 Ion evaporation from Taylor cones of propylene carbonate mixed with ionic liquids *J. Fluid Mech.* **591** 437–59
[46] Gañán-Calvo A M 1997 On the theory of electrohydrodynamically driven capillary jets *J. Fluid Mech.* **335** 165–88